HYDROGEN-POWERED INTEGRATED POWER AND PROPULSION SYSTEM (IPPS) ARCHITECTURE FOR SUSTAINABLE AVIATION: LEVERAGING SYNERGIES BETWEEN GAS TURBINE AND SOLID OXIDE FUEL CELLS

Diana San Benito Pastor
Safran SA
Paris, France

Evangelia Pontika
Cranfield University
Cranfield, UK

Stefanie de Graaf
German Aerospace Center
Cottbus, Germany

Daniel Ewald
Karlsruhe Institute of Technology
Karlsruhe, Germany

André Weber
Karlsruhe Institute of Technology
Karlsruhe, Germany

Stefan Kazula
German Aerospace Center
Cottbus, Germany

Mario L. Ferrari
University of Genoa
Genoa, Italy

Panos Laskaridis
Cranfield University
Cranfield, UK

ABSTRACT

Reducing aviation emissions requires innovative propulsion technologies. Hydrogen has been identified as a promising fuel to support the decarbonisation efforts in challenging industrial sectors, including aviation. Innovative architectures are needed to define advanced propulsion systems that can significantly enhance the overall efficiency of the system while eliminating CO_2 and reducing NOx emissions. To address this challenge, a propulsion system that integrates direct hydrogen combustion with fuel cell technology is proposed to create a tightly coupled system capable of effectively addressing these issues.

This paper presents the preliminary system architecture for a 1 MW+ Integrated Power and Propulsion System (IPPS) using hydrogen for a commuter application. It offers a methodology for defining an IPPS that leverages the synergies and benefits arising from the mechanical and thermodynamic coupling of a gas turbine (GT) with a solid-oxide fuel cell (SOFC) system. A review of SOFC technology explores its advantages and challenges in the context of GT integration. Based on literature review of GT-SOFC integration concepts, the paper outlines key design constraints and system requirements for the IPPS. A functional analysis defines the primary functions of the IPPS, i.e. propulsion, power generation, and power management, while an organic analysis identifies the physical components needed to comply with these functions and optimise their interactions within the system. Together, these analyses provide a detailed overview of the system's components and interfaces and define the IPPS baseline. The findings of this research will guide future progress toward decarbonised aviation solutions.

Keywords: Engine Performance, Turboprop, Hydrogen, SOFC, H_2 combustion

NOMENCLATURE

Acronyms

AC	Alternating current
APU	Auxiliary power unit
BoP	Balance of plant
DC	Direct Current
EGT	Exhaust gas temperature, K
EIS	Entry into service
FlyECO	Future enabLing technologies for hYdrogen-powered Electrified aero engine for Clean aviatiOn
FT	Free turbine
GT	Gas turbine
HEX	Heat exchanger
HPC	High-pressure compressor
HPT	High-pressure turbine
IPPS	Integrated power and propulsion system
LHV	Lower heating value, MJ/kg
MIC	Metallic interconnector
OPR	Overall pressure ratio, -
PMDS	Power management and distribution system
RGB	Reduction gearbox
SOFC	Solid oxide fuel cell
TET	Turbine Entry Temperature, K
TLAR	Top-level aircraft requirements
LPC	Low-pressure compressor
UAV	Unmanned aerial vehicles

Symbols

AU	Air utilisation, -
F	Faraday constant, 96485 As mol^{-1}
FU	Fuel utilisation, -
H	Molar specific enthalpy, kJ mol^{-1}
$\dot{H}$	Enthalpy flow, kW
I	Electrical current, A
$\widetilde{M}$	Molecular mass, g mol^{-1}
$\dot{m}$	Mass flow, kg s^{-1}
$\dot{n}$	Molar flow, mol s^{-1}
P	Pressure, atm
PW	Power, kW
T	Temperature, K or °C
U	Voltage, V
z	Number of exchanged electrons, -

Subscripts

AE	Air electrode
el	Electrical
FE	Fuel electrode
H_2	Hydrogen
H_2O	Steam
in	Inlet
O_2	Oxygen
out	Outlet
stack	SOFC stack

1. INTRODUCTION

Global greenhouse gas emissions must be significantly reduced to mitigate the escalating impacts of climate change. The aviation sector accounts for approximately 2-3% of global CO_2 emissions. Propulsion systems contribute 20–40% of historical emission reductions in aviation offering an additional 10–20% by 2050. Further reductions can be achieved adopting fuels like hydrogen (H_2), with potential for near-zero carbon output when derived from renewable energy sources.

It is in this context that the FlyECO project [1] [2], i.e. Future enabLing technologies for hYdrogen-powered Electrified aero engine for Clean aviatiOn, will deliver a transformative 1 MW+ Integrated Power and Propulsion System (IPPS) for a commuter application with the potential to enable aviation climate neutrality by 2050. The IPPS, solely running on H_2, comprises a gas turbine (GT) coupled to a Solid Oxide Fuel Cell (SOFC) system, namely a GT-SOFC, and aims to be more efficient than a classical GT for an equivalent entry-into-service (EIS). In addition to eliminating aviation CO_2 emissions entirely, injection of steam from the SOFC into the H_2-fuelled GT is expected to significantly reduce NO_X emissions.

Research on GT-SOFC architectures shows potential for efficiency and emission improvements. However, their aviation application faces challenges like system weight, thermal management, and fuel cell durability. The stringent safety and weight requirements in aviation further complicate adoption. While preliminary studies exist, more research is needed to address these barriers and optimise performance for commercial aircraft propulsion.

The IPPS baseline architecture in the FlyECO project aims for optimised integrated operation with a minimal number of components. A preliminary functional analysis identified key IPPS functions, power flows, and synergies between GT and SOFC subsystems. This article presents a methodology to define IPPS architectures, optimising system efficiency by leveraging both technologies' advantages, focusing on energy conversion, system complexity, and thermal management. The proposed framework aims to enhance propulsion system performance, fuel efficiency, and sustainability in aviation.

Even though the FlyECO project does not include aircraft design, a commuter reference aircraft with EIS 2050 and running on H_2 was defined to derive top-level aircraft requirements (TLAR) for the IPPS. For modelling the GT, a 1 MW propeller engine was initially chosen and virtually adapted to operate on H_2, with the initial assumption that it, along with another engine, would supply all the power needed for the aircraft. Initial SOFC analysis evaluated suitable technologies for the IPPS architecture. This led to a systems engineering approach to defining the baseline IPPS based on preliminary functional and organic analyses.

2. LITERATURE REVIEW

Aviation gas turbines operating in the 1 MW power class are usually turboprops, with about 30% overall efficiency. The FlyECO project explores IPPS architectures to improve the performance of the propulsion system through coupling a GT with an SOFC, exploiting their synergies and reducing emissions [3, 4, 5].

2.1. GT-SOFC Technologies

Proposals of SOFC-based hybrid systems in aircraft are not new for non-propulsive power generation. The potential of utilising SOFC and GT in a combined heat and power application is well known in stationary applications. Over the past few decades, a few potential configurations have been devised, examined, and assessed. The high operating temperature of the SOFC, resulting in high-quality waste heat, positions it as the most suitable fuel cell candidate for integration into a hybrid cycle.

In the late 1990s, Siemens Westinghouse pioneered a pressurised SOFC micro-GT generator hybrid power system, with a total electrical power output of 220 kW [6]. The initial trials of the hybrid power system demonstrated efficiencies of up to 52% on a lower heating value (LHV) basis.

In 1996, Bevc et al. [7] proposed three pressurised hybrid power plant configurations employing tubular, cathode-supported SOFCs from Westinghouse, with capabilities of 3 MW, 4.5 MW, and 10 MW. The 10 MW power plant incorporated an SOFC to a single-shaft GT downstream of a compressor and a heat exchanger (HEX), which operated as a recuperator. The SOFC generated over two-thirds of the overall alternating current (AC), resulting in a plant LHV efficiency of 60% of the natural gas fuel. The 3 MW and 4.5 MW layouts, both coupled to a two-shaft GT with a base LHV efficiency of ~43%, were enhanced by SOFC units. The 3 MW system's efficiency reached 61 % and the 4.5 MW system pushed efficiency to 67%.

In 2015, a literature review was conducted by Buonomano et al. [6] on stationary hybrid power plants, including an analysis of control strategies, alternative fuels, experimental studies, previous research and development, and market perspectives. The investigation revealed that most hybrid architectures were based on a pressurised system, where the SOFC is operated at a pressure level above atmospheric conditions to exploit the benefits related to an increase in Nernst voltage with increasing pressure and enhance the conversion efficiencies. One disadvantage of the pressurised configuration is the increased complexity and operational difficulties (e.g. regulate pressure discrepancies between the SOFC anode and cathode inlet). The scarcity of experimental data in most of the investigated studies can be attributed to the high capital costs and the low technology readiness level of this technology.

Research on SOFC-GT hybrids for aviation is limited. The SOFC high temperature operating conditions require long start-up/shutdown phases [8], and transient operation of SOFC-based hybrid systems must be analysed [9]. Waters (2015) [10] categorised them for unmanned aerial vehicles (UAV) and auxiliary power units (APU). Simulated UAVs for regional applications using H_2 fuel (20-140 kW) achieved a 66% system efficiency. The power range of the APUs was 200-440 kW with up to 74% system efficiency including fuel reformation. Different APU layouts were analysed in reference [11], highlighting the efficiency increase relative to the state-of-the-

art architectures. They are all hybrid systems with GT coupling to a pressurised SOFC to exploit the benefits related to the Nernst's voltage increase with pressure increase.

Wilson et al. (2022) [12] developed a model for an SOFC-GT hybrid power system, which presented a simulated total system efficiency of approximately 70% for a 1 MW system at an aircraft cruise altitude of approximately 11 km. In this system layout, the SOFC is located upstream of the combustor and generates approximately 62% of the total net electrical power [12]. Moreover, in the recent years it is important to highlight the design of an SOFC-based hybrid system for liquid fuels (Jet-A or Bio-Jet) [13] and a detailed integrated system using JP8 fuel converted in a catalytic partial oxidation (CPOx) reactor under different operational parameters [14]. Some dynamic analyses were also presented for a Cessna S550 Citation S/II aircraft [15].

Despite the extensive theoretical analyses, there has been a limited number of experimental studies. Companies, including Rolls-Royce Fuel and Mitsubishi, have developed SOFC-GT hybrid system prototypes, achieving total electrical efficiencies of approximately 50% [16, 17].

2.2. SOFC Technologies for Aviation

The vast majority of existing SOFC technologies have been developed for stationary applications. However, to use SOFCs in advanced aviation applications, the knowledge gained in the stationary sector over the past few decades can be used. Most of the more advanced technologies are further developments or modifications from those [18, 19, 20, 21], with some exceptions like 3D printed [5] or monolithic concepts [22].

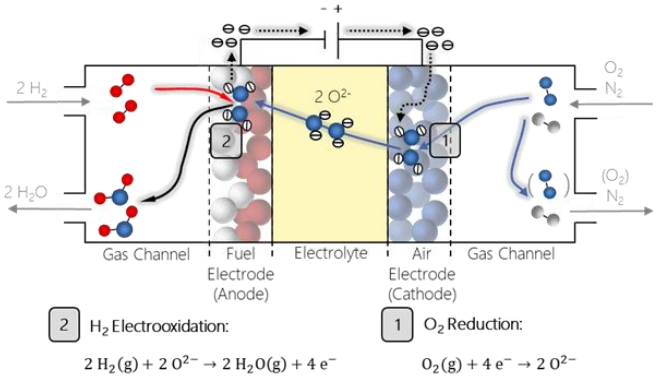

FIGURE 1: WORKING PRINCIPLE OF A SINGLE SOLID OXIDE FUEL CELL (SOFC)

To understand the potential of SOFC technologies for aviation, the working principle of an SOFC is shown in FIGURE 1 and described in detail by Singhal et al. [23]. Based on the operating conditions and the type of cell, a single cell can achieve a maximum power density of a few watts per square centimetre (W/cm^2). To achieve sufficient power, the cells are connected in series in a stack.

Cells are stacked together via interconnectors, also known as bipolar plates, that provide an electrical contact and a separation of the gas compartments between adjacent anode and cathode sides. The interconnector can be made of steel or conductive ceramics. The application of steel grades for metallic interconnectors (MICs) is economically beneficial since material and manufacturing costs are significantly lower compared to ceramic interconnectors (CIC) [24]. To transport fuel gas to the anode and air to the cathode side, these bipolar plates exhibit gas channels. Today´s stacks and sealing concepts are not designed to withstand elevated pressure levels in the range of several atmospheres. This makes it hard for the cell to operate under pressurised conditions. Thus far such operating conditions are usually achieved by using a pressure vessel – except for tests on single cell level [25].

For an aircraft application, a gravimetric power density on a system level of 0.7 – 2 kW/kg is required when coupling a gas turbine with an SOFC stack [26]. Increasing the power density could also be done increasing the operating pressure. However, the potential need of a pressure vessel also means more weight, which (at least partly) cancels out the increase in gravimetric power density.

Addressing these aspects, cell and stack concepts for an airborne application are presented in the following paragraphs. Current developments focus mainly on a cell and much less on a stack level, which is primarily due to the early stage of development for an application in the transportation sector. The manufacturing processes are therefore still on a laboratory scale and under development, which means that such cells are up to now commercially not available.

Planar stacks present the highest degree of maturity and commercialisation. A major advantage of planar stacks is that the internal resistance is relatively low, as the current is conducted perpendicular to the stack plane. However, sealing is rather challenging, as each cell must be sealed to the outside and glass sealants could lead to cell degradation over time. Gas tightness is mandatory to minimise fuel losses. Enhancing operating pressure, both with and without a pressure vessel, remains at the experimental stage [25]. Furthermore, MICs in planar SOFC stacks can take up to 70 % of the total stack weight [5], which may limit the ability of airborne applications to achieve high gravimetric power densities. The reduction of the weight is limited by the minimum thickness of the metal sheet used for MIC production.

To reduce the weight of the MIC, the monolithic cell and stack concept merges cell support, gas channels, and the interconnects into a single layer. This reduces stack heights by a factor of 2 – 4 compared to conventional planar SOFC stacks, enhancing both gravimetric and volumetric power densities [22]. The high metal content further reduces temperature gradients across the stack during operation. This makes the stack more resilient to quick temperature changes, which is crucial for handling sudden power shifts and quick starts, typical in aircraft operations. Such a monolithic stack exhibits a power density of 5.6 kW/L, whereby values of 6 – 8 kW/L appear to be feasible. It is expected that the costs for these stacks will be lower than traditional ones due to the reduced thickness and use of cost-effective metals like iron. However, the manufacturing process is challenging as it requires the sintering of various ceramic and

metallic parts in a H_2 atmosphere while maintaining a hierarchical microstructure for the main gas flows and gas diffusion paths. There is uncertainty about the long-term durability of this design, as the thin gas channels may not resist corrosion well. Additionally, the most complex part of the process is the binder burnout, which restricts the number of repeating units in a single stack. Despite these challenges, a monolith has been successfully produced and tested at the single repeat unit (SRU) level. [22]

Siemens Westinghouse previously developed a monopolar tubular cell concept for stationary applications. Thereby, the cell corresponds to a tube with inner diameters of >10 mm and the porous cathode on the inside being the support. Serial/parallel contact between the cells is realised by ceramic interconnectors and nickel felts on the outside, leading to a so-called tube bundle reactor. Long-term operation over 70,000 h has proven durability [19]. Such a tubular SOFC stack with an electrical power output of 176 kW was successful in coupled operation with a micro-GT (47 kW_{el}), achieving an electrical net efficiency of 57 % [18]. For this, a pressurised operation up to 3 atm was realised by integrating the stack in a pressure vessel [3]. A major advantage of the tubular concept is that the anode and cathode are already separated through the intrinsic cell geometry. This leads to a straightforward sealing procedure, where only the in- and outlet of tubes and the fuel gas compartment need to be sealed. In addition, the ends of the tubes are commonly in a rather "cold" region, which further simplifies the flexible attachment of the tubes. However, in-plane ohmic losses are higher due to longer current paths compared to planar cells, which leads to a lower power density [19].

The idea to decrease the diameter of tubular cells to enhance power density is pursued by several research groups and companies. The power density scales with the reciprocal of the tube diameter [27]. Such micro-tubular cells exhibit diameters of 2 – 5 mm [27], resulting in a compact and lightweight design. On a single cell level, a gravimetric power density of 2 kW/kg has been recently reported [5]. As the thermal mass of such a lightweight cell is lower than in planar cells, the thermal shock resistance is remarkably increased, which allows micro-tubular SOFCs to be started from ambient temperature within a few minutes. However, it is rather challenging to integrate the required large number of microtubular cells into a stack and collect the current generated along the cell. The in-plane resistance of the electrodes / current collector layers limits the maximum length of such cells.

Through a segmental arrangement of the cells along the pipe, current collection losses can be significantly reduced. Such a networking concept is also feasible for planar cells. The surface is split into several compartments, which are electrically connected with each adjacent. Through this, the current paths are shorter and therefore the ohmic resistance lower. However, the manufacturing process is challenging in terms of sealing, as the functional layers are overlapping to each other. [21, 5, 28]

Instead of using a cathode or ceramic support as it was earlier done by Siemens Westinghouse or Mitsubishi Heavy Industries for tubular cells, metal, anode- and electrolyte-supports are being targeted for micro-tubular cells [5, 27]. In general, anode-supported SOFCs can provide significantly higher power density values compared to electrolyte-supported ones, as the thickness of the electrolyte can be reduced, which results in a lower ionic resistance for the oxygen (O_2) transport and increases the cell performance [29, 30]. In addition, the operating temperatures can be decreased. However, conventional extrusion processes result in tube wall thicknesses that are limiting the gas diffusion of the fuel, leading to an increased polarisation resistance [18]. Electrolyte-supported cells are usually operated at higher temperatures above 1073 K or 1173 K (800 °C or 900 °C) to reduce more pronounced ohmic losses resulting from the thicker electrolyte. Fabrication methods for electrolyte-supported micro-tubular cells are more complex compared to anode-supported ones [31]. In general, the manufacturability of thin electrolyte layers is key to achieve high gravimetric power densities [5]. Recent progress in 3D ceramic printing technologies seems to make electrolyte-supported lightweight cells, at least on a laboratory scale, feasible [5].

The 3D ceramic printing technology is not only restricted to micro-tubular cells, for example 3D printed ceramic gyroid structures can be produced. Numerical simulations with state-of-the-art electrode and electrolyte (100 – 200 µm thick) configurations predict gravimetric power densities for such gyroid structures of 1.5 – 10 kW/kg on a cell level between 700 – 900 °C. However, stack connection of gyroid cells presents electrical connection and gas distribution challenges. [5]

Recent developments in cell technology are showing promising outcomes in terms of both gravimetric and volumetric power densities. These advancements also seem to align with critical aircraft operational needs, including the ability to handle rapid load changes and resist thermal shock, at least in laboratory settings. However, the long-term durability of these cells remains a question. Research is ongoing into how these cells can be effectively scaled up into larger stacks. Moreover, there's a need for further refinement of the manufacturing processes, not only for optimisation purposes but also to enable mass production in the future.

3. METHODOLOGY

The IPPS represents the propulsive system and must be designed as a whole, with its thermodynamic cycle encompassing the GT and the SOFC. The technology selection for the IPPS subsystems represents the technology level expected in 2050. The IPPS comprises three main subsystems: the GT, the SOFC stack, and the balance of plant (BoP), which is shared between the GT and the SOFC and must be defined to enable and enhance the synergies between them.

To fully benefit from the GT-SOFC coupling and enhance the IPPS overall performance, both thermodynamic and mechanical hybridisation are required. Thermodynamic hybridisation involves injecting all the output products of the SOFC into the GT combustor, contributing to the enthalpy rise in the combustor and reducing NOx emissions. Mechanical hybridisation refers to using the electricity produced by the SOFC to contribute to the IPPS propulsive power.

The studied IPPS fulfils two main service functions: generating propulsive power and generating (electrical) power for non-propulsive systems.

3.1. Definition of IPPS Requirements

Before delving into the functional analysis of the IPPS system or imagining potential coupling solutions between the GT and the SOFC, it is crucial to understand the top-level aircraft requirements (TLAR) and the orders of magnitude of the key performance parameters for the IPPS components. An H_2 commuter (19 PAX) aircraft application was chosen as use case to develop a 1 MW+ IPPS. The TLARs for a baseline aircraft mission specification are presented in TABLE 1.

TABLE 1: BASELINE FLYECO AIRCRAFT TLARS

Range	500 nm
(Auxiliary range)	(240 nm)
Number of passengers	19
Cruise speed	220 – 275 knots
Maximum altitude	25000 ft
(one engine inoperative)	(16000 ft)
Take-off power per engine	954 kW

3.2. The Gas Turbine

The baseline H_2 turboprop engine features a single spool and a free turbine shaft. It incorporates a three-stage low-pressure axial compressor (LPC) alongside a single-stage high-pressure centrifugal compressor (HPC). The engine utilises a reverse flow combustor. Its high-pressure turbine (HPT) has a single axial stage, while the free turbine (FT) comprises two stages. The FT shaft is linked to a gearbox, which has a reduction ratio of 17.58, driving a propeller at a full rotational speed of 1700rpm.

To explore the synergies between the GT and the SOFC, and define an IPPS architecture, a thermodynamic model on the GT with no integration with the SOFC was created first. The topology diagram of the GT core is presented in FIGURE 2 and follows the layout described previously.

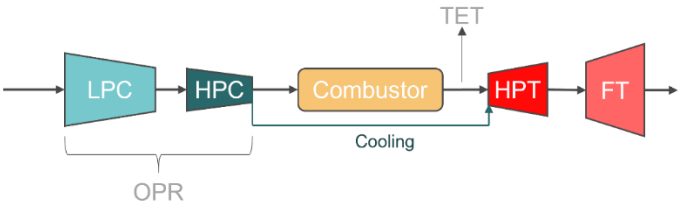

FIGURE 2: TOPOLOGY DIAGRAM OF THE BASELINE GAS TURBINE CORE

The GT performance simulations are performed in Turbomatch, Cranfield University in-house engine simulation code [32] [33]. It is a component-based tool that resolves the operating parameters of the engine at design and off-design points based on component maps, thermodynamic calculations, conservation of energy, and conservation of mass. The fundamental equations and methods for GT performance analysis are well-documented in reference textbooks, e.g. [34].

Gas turbine design point parametric analyses were performed using the overall pressure ratio (OPR) and turbine entry temperature (TET) as the thermodynamic cycle design parameters to produce the carpet plots shown in FIGURE 3 and FIGURE 4. Both cruise and take-off are treated as design points in this exploration. After the design is fixed, the OPR is allowed to vary based on the off-design point simulation.

For every set of TET and OPR, there is a unique mass flow that results in the target output power. The initial assumptions used in the modelling of the baseline H_2 GT engine are summarised in TABLE 2.

TABLE 2: BASELINE GT MODELLING ASSUMPTIONS

Cold Section	**LPC Efficiency**	0.85
	HPC efficiency	0.85
	HPC PR	2.1
	HPC/LPC Surge Margin	0.85
	Cooling Fraction to the HPT	5%
Hot Section	**Combustor Pressure Loss**	5%
	HPT efficiency	0.87
	FT efficiency	0.87

Assuming the air for the SOFC comes from the HPC outlet, four performance parameters have been identified to explore potential synergies and feasible interfaces with the SOFC:

1. The **HPC outlet pressure ($P_{HPC,out}$)**, which should ideally fall within the SOFC's operational limits.
2. The **HPC outlet temperature ($T_{HPC,out}$)** , which should also be within the SOFC's acceptable range.
3. The GT **airflow**, which indicates the total airflow going through the GT core, from which bleed air can be diverted to the SOFC to comply with the SOFC requirements.
4. The **exhaust gas temperature (EGT)**, at the FT exhaust, is a potential additional heat source for the SOFC air preheating.

The thermal efficiency is also a parameter of interest as one of the goals for the IPPS is to achieve an overall efficiency beyond the efficiency of the GT alone, as defined by Eq. (3-1).

$$\eta_{GT,therm} = \frac{PW_{GT}}{\dot{m}_f \cdot LHV} \tag{3-1}$$

The design point cycle analysis and combinations of TET and OPR for a fixed target nozzle outlet pressure ratio are presented in FIGURE 3 for take-off and in FIGURE 4 for cruise conditions and power.

At take-off conditions a GT with OPR of 10 can deliver bleed air (HPC outlet) at 604 K (FIGURE 3c) and 10 atm. The minimum inlet temperature of the SOFC is 600 °C (873 K). Therefore, there is a ~270 K gap to be bridged before the bleed air is suitable for the SOFC. Additionally, the bleed air to the SOFC must meet the pressure requirements of the SOFC. A combination of SOFC technology developments with higher

operating pressure, BoP design and GT design solutions along with control strategies needs to be explored to enable these two components to work together and within their operating ranges.

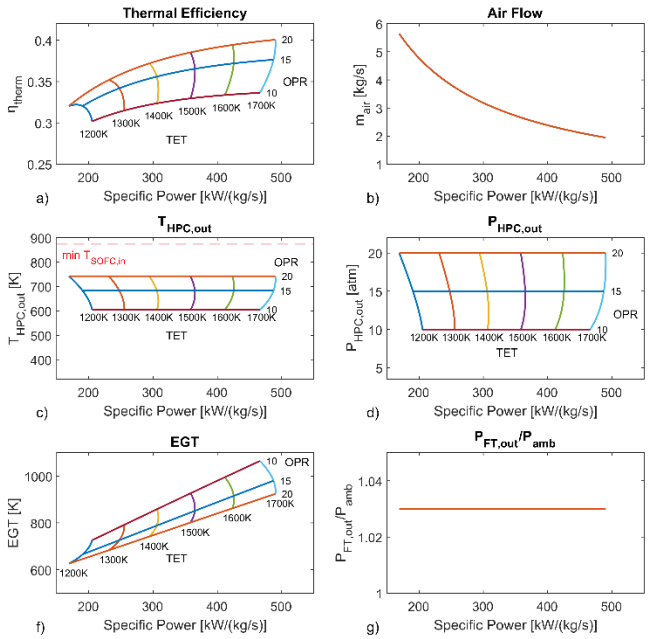

FIGURE 3: THERMODYNAMIC ANALYSIS OF GT DESIGN POINT AT TAKE-OFF (ALT=0, MN=0, PW=954 KW)

At cruise conditions, the gap between HPC outlet temperature and minimum SOFC inlet temperature further increases as the ambient temperature has reduced at cruise altitude (FIGURE 4). For OPR = 10, the HPC outlet temperature is 520 K. Therefore, the gap to the minimum inlet temperature of the SOFC becomes ~350 K. The in-flight variations of GT operating conditions exhibit one of the main challenges for coupling GT with SOFC and is linked to the question of SOFC durability and performance under temperature and pressure gradients during climb and descent, as well as other transients such as transitioning from GT ground idle to full power at take-off. Attention should be given on how these temperature and pressure variations are managed in an IPPS with GT and SOFC.

Another parameter to consider is the air flow. The higher the TET, the higher the specific power. Therefore, for a set power output the GT airflow will reduce (FIGURE 3b and FIGURE 4b). In the hybrid GT, the power contribution from the GT will reduce due to the mechanical hybridisation and, therefore, the airflow of the GT for a set specific power and TET is expected to further reduce. This initial airflow estimation will help assess if the GT air can offer sufficient bleed air to the SOFC. Furthermore, mechanically hybridising and further downsizing an already small baseline GT engine may start introducing turbomachinery performance constraints due to lower Reynolds numbers and higher tip clearance losses.

The baseline H_2 GT thermodynamic exploration identifies possible conditions and starting points to evaluate interfaces with the SOFC. It also defines feasible architecture solutions and necessary auxiliary components for a shared BoP. However, it should be noted that when the GT is integrated with the SOFC, its operating point will change and some of the operating parameters are expected to move to different values along with refining the initial assumptions based on the new GT design.

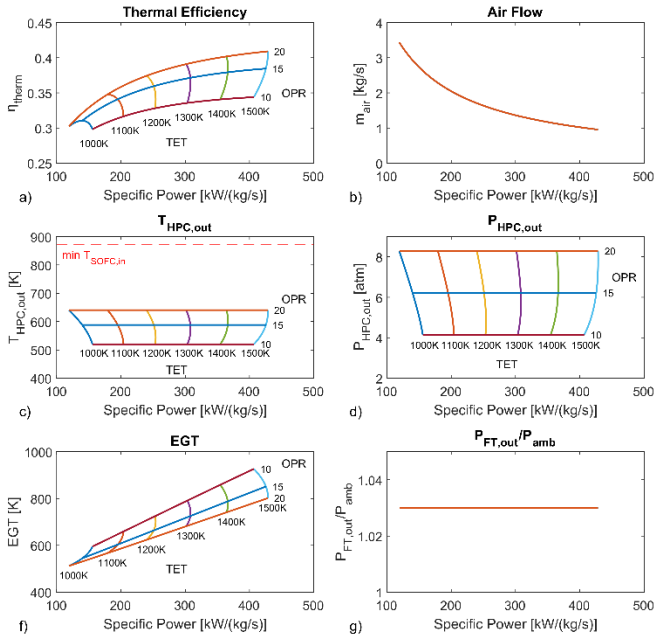

FIGURE 4: THERMODYNAMIC ANALYSIS OF GT DESIGN POINT AT CRUISE (ALT=25 kFT, MN=0.4, PW=409.5 KW)

3.3. The SOFC

To evaluate the suitability of SOFC technologies in the IPPS environment and define their mass flow requirements, an analysis was carried out based on the mechanical degree of hybridisation of the IPPS, which represents the contribution of the SOFC to generating propulsive power relative to the total propulsive power output of the IPPS. Thereby, the electrical power output of the SOFC powertrain has been varied between 10 % and 50 % of the GT power output, as defined by its maximum power conditions, i.e. at take-off.

The electrical power output of an SOFC stack $PW_{\mathrm{el,SOFC}}$ depends on the operating stack voltage U_{stack} and overall current I, since $PW_{\mathrm{el,SOFC}} = U_{\mathrm{stack}} \cdot I$. Assuming one stack with a parallel connection of all cells, U_{stack} equals to the cell voltage U_{cell}. According to Faraday's law, the overall current is directly proportional to the converted amount of H_2 or O_2. Then, a mass flow $\dot{m}_i$ of converted H_2 or O_2 can be calculated according to equation (3-2) with the molecular mass $\widetilde{M}_i$, number of exchanged electrons z, and Faraday constant F.

$$\dot{m}_{i,conv} = \widetilde{M}_i \cdot \frac{PW_{el,SOFC}}{U_{cell} \cdot z \cdot F} \qquad (3\text{-}2)$$

The overall mass flows $\dot{m}_{\mathrm{tot}}$ at the air electrode (AE) and fuel electrode (FE) are defined by the conversion, which is

usually specified as fuel utilisation (FU), i.e. Eq. (3-3), for the fuel side and air utilisation (AU) , i.e. Eq. (3-4), for the air side.

$$FU = \frac{\dot{m}_{H_2,in} - \dot{m}_{H_2,out}}{\dot{m}_{H_2,in}} \tag{3-3}$$

$$AU = \frac{\dot{m}_{O_2,in} - \dot{m}_{O_2,out}}{\dot{m}_{O_2,in}} \tag{3-4}$$

With this, the required total mass flow at the fuel side, i.e. Eq. (3-5) solely with H_2, and air side, i.e. Eq. (3-6), can be calculated, whereby an additional factor of $1/0.21$ for the air side needs to be introduced since air contains 21 % O_2.

$$\dot{m}_{FE,tot} = \frac{\dot{m}_{H_2,conv}}{FU} \tag{3-5}$$

$$\dot{m}_{AE,tot} = \frac{1}{0.21} \cdot \frac{\dot{m}_{O_2,conv}}{AU} \tag{3-6}$$

Typically, a cell voltage of 0.7 V is used for benchmarks since this operating point lays at relatively high-power densities. Even though the cell voltage depends on the specific flight mode, such a cell voltage is assumed initially for the IPPS.

To further explore SOFC design parameters, a black box model has been set up, which is based on an enthalpy balance of inlet and outlet gas streams and the electrical power output calculated by means of equation (3-2) Assuming an adiabatic operation and the same outlet temperature on both the anode and cathode side, equation (3-7) results with the molar specific enthalpy flow $\dot{H}_i = \dot{n}_i \cdot H_i = f(T)$. Molar specific enthalpies H_i were included by using NIST polynomials [35] and $\dot{n}_i$ corresponds to the molar gas flow. Since, $\dot{H}_i \sim PW_{\mathrm{el,SOFC}}$ and consequently, $PW_{\mathrm{el,SOFC}}$ is reduced in Eq. (3-7).

$$(\dot{H}_{FE,in} - \dot{H}_{FE,out}) + (\dot{H}_{AE,in} - \dot{H}_{AE,out}) = PW_{el,SOFC} \tag{3-7}$$

Based on this, the outlet temperature T_{out} can be calculated for given inlet parameters. These were pre-defined in a physically meaningful range. The inlet temperature T_{in} has been varied between 600 °C and 800 °C and the cell voltage between 0.6 and 1.1 V. Regarding the amount of gas conversion, FU lays in between 0.1 and 0.8 and AU ranges from 0.1 to 0.6. To account for thermomechanical stresses due to temperature gradients from the inlet to the outlet, a maximum $\Delta T = T_{\mathrm{out}} - T_{\mathrm{in}}$ of 250 K was set as a limit for the outlet temperature.

The results of the preliminary SOFC design space exploration are presented in FIGURE 5. It shows three-dimensional design diagrams of the SOFC as an output of the parametric sweep. While the FU exhibits a relatively low sensitivity towards ΔT, AU turns out to be a significant turning knob to control the temperature increase.

This methodology is useful for exploring specific operating points which might be of interest for an SOFC-GT coupling on a thermodynamic level. However, it should be noted that it does not consider the type of SOFC cell or stack used and with this no specific power density at the respective operating point.

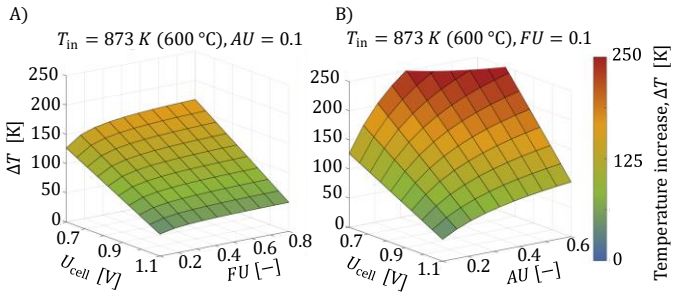

FIGURE 5: EXEMPLARILY PARAMETRIC SWEEP OF A) U_{cell} AND FU AT $AU = 0.1$ AND B) U_{cell} AND AU AT $FU = 0.1$.

4. PRELIMINARY FUNCTIONAL ANALYSIS

Based on the parametric analyses undertaken for the GT and the SOFC, the requirements of the IPPS have been identified, and a preliminary functional definition of the system can be conducted. A preliminary functional analysis for a new propulsion system involves identifying and outlining the system's primary functions and subfunctions. Functions are the essential tasks or operations that the system or its components are designed to perform, contributing to the overall performance and objectives of the propulsion system. This analysis ensures that the IPPS meets performance, safety, and efficiency requirements before detailed design.

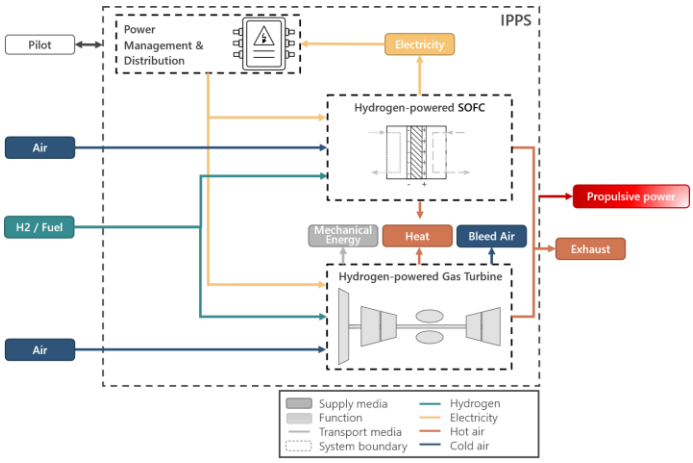

FIGURE 6: CONTEXT DIAGRAM FOR DEFINITION OF THE MAIN FLOWS IN THE IPPS

The IPPS system has three main functions: converting fuel to mechanical power, generating electrical power, and supplying air bleed. The latter will remain unchanged and is not addressed in this study. These functions are very high-level and require further definition of subfunctions and flows. Since the aim of the study is to enhance GT-SOFC synergies, identifying power flows between the functions is essential. These macro-level power flows, presented in FIGURE 6, include fluid flows of air and H_2 fuel into the GT and SOFC stack, potential synergy fluxes

between the GT and SOFC to address excess heat generated by inefficiencies in the GT or the SOFC, electricity produced by the SOFC, and conventional aircraft requirements of air bleed for the environmental control system or mechanical energy for ancillary systems. Additionally, there are exhaust products from the GT or SOFC that contribute to the overall propulsive power generated by the IPPS.

The direction of flows in FIGURE 6 may change depending on the operational situations. Understanding the potential behind these power flows enables the definition of key parameters and operation modes of the IPPS architecture. The propulsion system interface is defined by the dotted lines in FIGURE 6.

The simplified context diagram in FIGURE 6 allowed the identification of the primary functions that the IPPS sub systems would need to address, as presented in FIGURE 7. The modelling of the fuel system is outside the scope of the FlyECO project, and the fuel flow reaching the IPPS interface is assumed to be at the required conditions, as defined by the GT combustor. There might be a mismatch with the fuel inlet requirements at the SOFC stack, further exacerbated during some phases of flight. Therefore, additional conditioning requirements inside the IPPS perimeter are considered in the definition of the IPPS architecture. Furthermore, the electrical interface will be sized to comply with the needs specified in ATA24, and the air bleed interface will comply with existing ATA36, ensuring appropriate air bleed to the aircraft.

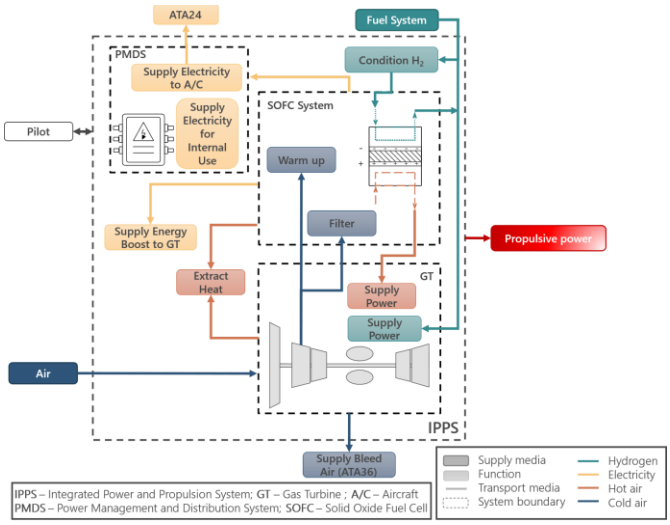

FIGURE 7: IPPS SYSTEM FUNCTIONAL DEFINITION

The SOFC anode inlet requirements are addressed by the "Condition H_2" function. The temperature of H_2 entering the SOFC unit would be higher than the temperature of the H_2 directly injected into the combustor, necessitating the warming up of the anode inlet flow. The flow pressure difference entering the SOFC anode and cathode needs to be less than 100 mili-atm, depending on the cell technology and stack architecture, thus requiring pressure control.

In FlyECO, the SOFC cathode air flow to the SOFC unit comes from the compressor. The temperatures of the flows entering the cathode and the anode of the SOFC should be equal. The air flow in the compressor would reach a maximum temperature of 604 K, while the inlet temperature to the SOFC would be around 873 K. Therefore, a "Warm Up" function is necessary between the GT compressor and the SOFC inlet. Additionally, it has been shown that pressures above 10 atm do not significantly benefit SOFC efficiency [36]. This pressure is attainable throughout the flight mission by the GT compressor, and no specific function is yet defined for controlling the pressure.

FIGURE 7 shows that both the GT and the SOFC stack unit have heat losses, that require a “Extract Heat” function. These losses could, therefore, be used to address the “Warm up” demands mentioned above.

The electricity generated by the SOFC unit serves three subfunctions: supplying electricity to the aircraft (ATA24), providing electricity for internal usage of the IPPS, and supplying a power boost to the GT. The FlyECO project baseline hypothesis suggests that this power boost is delivered directly at the reduction gearbox (RGB), leading to a reduction of the GT power requirement while maintaining the same propeller thrust of power requirements, and hence a reduction in the core size.

The outlet products of the SOFC go into the GT combustor and complement the power supply requirements that would conventionally be addressed by the fuel line. This contribution is represented by the “Supply Power” function. This thermodynamic contribution of the SOFC would define the thermodynamic hybridisation of the IPPS, i.e. the power contribution of the thermodynamic products from the SOFC relative to the H_2 injection directly from the fuel system.

Finally, the air bleed requirements (ATA36) defined by the aircraft specification are also considered.

An additional function identified for the SOFC stack in FIGURE 7 is the "Filtering" function, which ensures the removal of sulphur and other contaminants. The FlyECO project baseline assumes that the cathode air reaching the SOFC could contain some water, but the molar fraction would be below an acceptable threshold, so a "To Dry" function has not been added. This hypothesis will be explored further in the project to quantify the SOFC stack's tolerance to humidity, considering conditions such as rain. For an SOFC stack with EIS 2050, the FlyECO project baseline assumes that a "Gas tight" concept is acceptable up to 10 atm, avoiding the need for a heavy pressure vessel or metal enclosure.

The function depiction in FIGURE 7 represents the nominal functioning of the IPPS. Additional functions might be required for addressing the entire mission envelope. However, the nominal functioning of the system should be evaluated before consideration of abnormal modes of operation.

5. PRELIMINARY ORGANIC ANALYSIS

The functional analysis approach described before sets the working ground for the preliminary organic analysis and the definition of components, and their interconnections within the IPPS system. An organic analysis involves defining components to address the tasks identified by the functions in the preliminary

functional analysis. The goal of the organic analysis is to maximise IPPS performance while minimising system complexity. Therefore, the functions identified in FIGURE 7 have been transposed to an organic definition diagram, where possible organic solutions are identified (FIGURE 8).

Even though the fuel conditions at the interface between the fuel system and the IPPS have been assumed to match the requirements of the GT combustion chamber, there is a need for a metering valve to control the fuel flow entering the combustor.

It should be noted that the control architecture will be defined at a later stage in the project. Therefore, the functions corresponding to the different control aspects of the IPPS subsystems are not considered in the definition of the IPPS baseline (FIGURE 7), and the initially proposed components might be modified to accommodate the control needs, for example, instead of a metering valve, a three-way-valve might be deemed more suited in future studies.

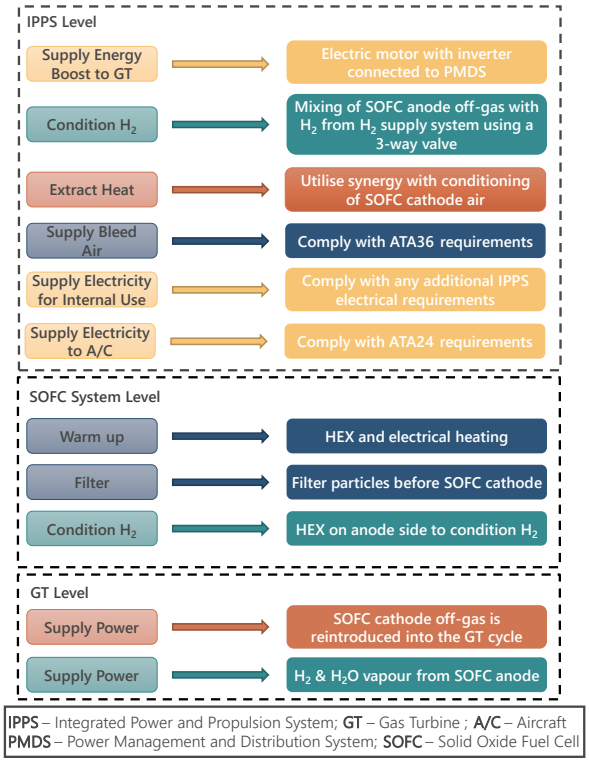

FIGURE 8: ORGANIC DEFINITION OF THE IPPS

The electricity generated by the SOFC will be managed differently based on the subfunctions it addresses. It will be directed to a power centre to supply electricity to the aircraft (ATA24) and its control system. Additionally, the power centre, potentially combined with the previous function, will supply electricity for the internal usage of the GT and its control system. Furthermore, an electric motor, thermal management system, and power electronics will be required to provide an energy boost to the RGB, subsequently impacting the GT.

The SOFC anode inlet requirements, addressed by the "Condition H_2" function, are fulfilled through several means. A HEX is used to warm up H_2 to the required temperature at the IPPS interface to ensure ideal operating conditions for the SOFC. The airflow pressure entering the SOFC anode is initially assumed to match the pressure going into the GT combustor, so no additional component is required at this stage. However, an additional compressor might be needed to ensure operability and could be explored in future iterations of the IPPS architecture. Lastly, the fuel flow entering the SOFC is controlled by a valve.

Regarding the outlet conditions of the SOFC products, the underlying assumption is that the pressure losses generated by the ancillary systems between the air extraction from the compressor and its reinjection in the GT combustor are equivalent to the pressure losses between the compressor exit and the GT combustor inlet. Numerical trade-offs are required to evaluate whether this approach is beneficial relative to including an additional compressor to pressurise the SOFC outlet products from cathode and anode to ensure operability.

The SOFC cathode air flow to the SOFC unit comes from the compressor, according to the FlyECO project hypothesis, and requires additional components. A HEX followed by an electric heater is needed to warm up the air extracted from the GT compressor to the required temperatures for correct SOFC operation. The airflow pressure entering the SOFC cathode should be managed by the control system, will be defined at a later stage of the project, so no specific component is included in the IPPS baseline for this purpose. Within the SOFC stack unit, the airflow is filtered and then injected into the SOFC cathode.

6. IPPS BASELINE

The baseline architecture for the FlyECO IPPS (FIGURE 9) is the outcome of the preliminary functional and organic analyses presented before for the nominal operating condition of the IPPS. Abnormal cases of operation have not yet been evaluated. The architecture in FIGURE 9 is the point of reference for current analyses in the FlyECO project and for future IPPS iterations.

The SOFC system is mechanically coupled to the shaft driving the IPPS propeller via a power management and distribution system (PMDS). The FT of the GT is connected to the gearbox to ensure this coupling. On the IPPS-level a thermal management system (TMS) is required to for maintaining ideal operating temperatures in the electrical components. The PMDS consists of an electric motor and its inverter, solid-state switches, and potentially it also includes DC-DC-converters to condition the voltage level of the SOFC system to the distribution bus voltage level.

The thermodynamic cycle of the IPPS baseline is the combination of a classical GT Brayton cycle and the addition of the waste heat produced by the SOFC to the GT combustor, thereby creating a topping cycle. An ideal temperature-entropy (T-s) diagram is shown in FIGURE 10 to illustrate the potential of utilising the additional energy contribution from the SOFC thermodynamic outputs to produce propulsive power. There is a portion of the GT compressed air, which goes directly to the combustor, while another is diverted to the SOFC. The output products of the SOFC are then introduced in the GT combustor, contributing energy. Station 3.1 indicates the location where the

hotter SOFC products are mixed with the "cooler" GT main flow, and hence the temperature jump from the exit of the HEX hot side to the station 3.1, which is the combustor inlet. In reality, the individual processes are associated with irreversible losses such that one cannot assume them to be isentropic, and the heat addition/removal processes along the P3 curve are not isobaric.

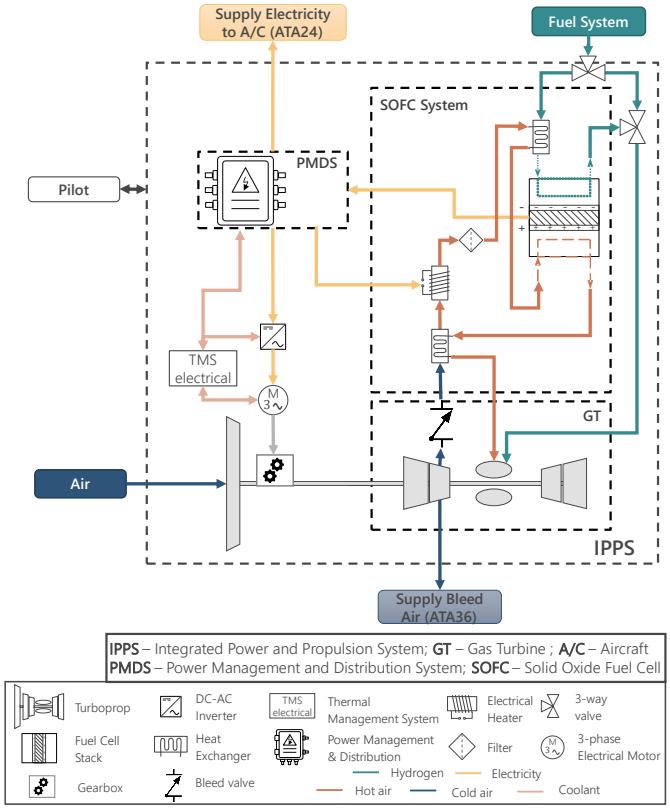

FIGURE 9: IPPS BASELINE ARCHITECTURE

Zooming into the SOFC system in FIGURE 9, the SOFC is operating in pressurised mode. The air into the SOFC cathode comes from the GT compressor. The need to increase the reactant temperature to values in the range of 600-800 °C (depending on the SOFC technology), the air flow rate is pre-heated with a HEX able to exploit the thermal content at the SOFC outlet (cathodic side). An electrical heater placed after the HEX could also be included for specific operations. A second heat exchanger has been installed for H_2 pre-heating upstream of the anode inlet. This ensures equal temperatures between the anode and cathode inlets. While in FIGURE 9 this device uses the thermal content of the air flow, other solutions could be considered. Finally, the SOFC exhaust products are reintroduced in the GT combustor: unused H_2, steam and cathodic air. Steam injection contributes to NOx mitigation can be obtained in the combustor.

Due to the light-weight target for aircraft applications, special attention was devoted to the system components. For instance, heat exchangers, although proposed in some works [37] [14] for integration simplicity, could introduce too much additional weight (especially if designed for high effectiveness performance). So, the application of single stage ejectors could present important benefits for air preheating upstream of the cathodic side [38]. Moreover, the application of a start-up burner (instead of an electrical heater) is considered a promising solution for coupling flexibility and weight decrease [39].

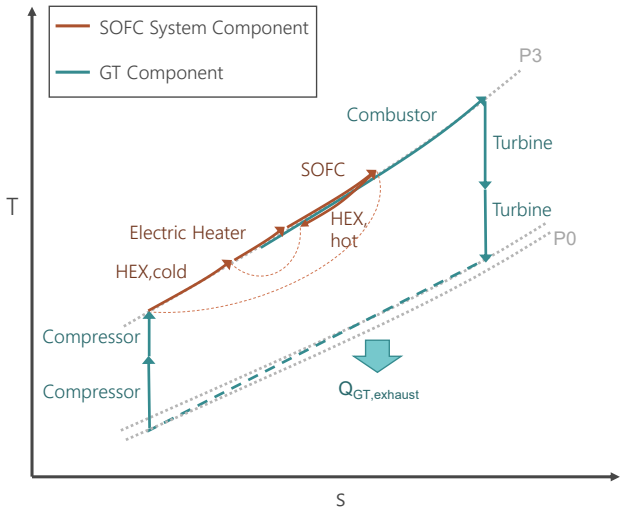

FIGURE 10: IDEALISED T-s DIAGRAM OF THE IPPS

7. CONCLUSION

The methodology presented in this research outlines the steps for defining the IPPS architecture for propelling a 19-passenger commuter H_2 aircraft, focusing on operating modes, orders of magnitude, and preliminary functional and organic analyses. The IPPS baseline defines the initial propulsive architecture for the FlyECO project. The synergetic benefits from GT-SOFC coupling present high potential to significantly reduce specific fuel consumption and mission fuel burn of the IPPS compared to a H_2 GT with EIS2050, while reducing NOx emissions.

The assessment of the baseline H_2 GT interfaced to the SOFC at take-off and cruise revealed a mismatch in the operating temperature between 270 K and 350 K lower than the SOFC minimum inlet temperature requirement. At take-off conditions, the GT bleed air pressure far exceeds the operating limit of today's SOFC. These results define a design space for the GT that is compatible with SOFC coupling. Additionally, the evaluation of SOFC stack designs and the outcomes of SOFC simulation models ratify their potential for airborne applications, with EIS2050. However, these preliminary analyses also showed that SOFCs for aircraft propulsion require a significant increase in their gravimetric power. This will be further explored in the FlyECO project as the SOFC is an IPPS technology enabler.

The mechanical and thermodynamic integration of a GT with an SOFC for synergetic generation of propulsive power in an aircraft is a disruptive concept. The mechanical integration (also known as electrical hybridisation) will reduce the power demand of the GT for complying with the propelling requirements of the IPPS. The thermodynamic integration of the SOFC into the GT cycle exploits three main thermodynamic synergies between these two subsystems:

1. Using pressurised and preheated bleed air from the GT compressor to feed the SOFC cathode avoids additional mass, volume and complexity of an additional auxiliary compressor to feed the SOFC.
2. The GT bleed air serves as heat sink for the SOFC, and reintroducing this air to the GT combustor contributes additional energy and may result in an overall reduction in H_2 flow to IPPS.
3. Injecting SOFC outlet steam in the GT combustor contributes additional energy to the cycle, improves GT thermal efficiency [40], and reduces NOx production.

The definition of the IPPS baseline is crucial for establishing the preliminary global control logic for the IPPS. These efforts lay the groundwork for future explorations of the IPPS design space. The IPPS topology definition will be refined based on inputs from the GT studies, SOFC stack design modelling, BoP modelling and thermal management strategies, and control strategies. A combination of design and control solutions between the GT and BoP will be required for pressure and temperature regulation to ensure SOFC performance, integrity and durability, as well as for the IPPS.

The evolution of the IPPS architecture towards enhanced performance will be realised through the collaborative efforts within the FlyECO project. This collective endeavour is key to defining and refining an IPPS architecture that is not only improved relative to future H_2 GT, but also optimised for peak efficiency.

ACKNOWLEDGEMENTS

Co-funded by the European Union

This project has received funding from the European Union's Horizon Europe research and innovation programme under grant agreement N° 101138488. It has also received funding from UK Research and Innovation (UKRI) under grant agreement 10106893.

REFERENCES

[1] "Future enabLing technologies for hYdrogen-powered Electrified aero engines for Clean Aviation," [Online]. Available: https://flyeco-european-project.eu. [Accessed the 2 December 2024].

[2] European Commission, "CORDIS - EU Research Results: Future enabLing technologies for hYdrogen-powered Electrified aero engine for Clean aviatiOn," [Online]. Available: https://cordis.europa.eu/project/id/101138488. [Accessed the 2 December 2024].

[3] M. L. Ferrari et al., Hybrid Systems Based on Solid Oxide Fuel Cells, John Wiley & Sons Ltd, 2017.

[4] M. A. Azizi and J. Brouwer, "Progress in solid oxide fuel cell-gas turbine hybrid power systems: System design and analysis, transient operation, controls and optimization," *Applied Energy,* vol. 215, p. 237–289, 2018. doi: 10.1016/j.apenergy.2018.01.098.

[5] P. Nehter et al., "Solid Oxide Fuel Cells for Aviation," *ECS Transactions*, vol. 111, n° 6, p. 143–154, 2023. doi: 10.1149/11106.0143ecst.

[6] A. Buonomano et al., "Hybrid solid oxide fuel cells–gas turbine systems for combined heat and power: A review," *Applied Energy,* vol. 156, p. 32–85, 2015.

[7] F. Bevc, W. L. Lundberg and D. M. Bachovchin, "Solid Oxide Fuel Cell Combined Cycles," in *Proceedings of the ASME 1996 International Gas Turbine and Aeroengine Congress and Exhibition*, Birmingham, UK, 1996. Paper No: 96-GT-447, V003T08A012. doi: 10.1115/96-GT-447.

[8] M. L. Ferrari et al., "Control system for solid oxide fuel cell hybrid systems," in *Proceedings of the ASME Turbo Expo 2005*, Reno, NV, USA, 2005. Paper No: GT2005-68102, pp. 55-63. doi: 10.1115/GT2005-68102.

[9] T. Brinson, J. Ordonez et C. Luongo , "Optimization of an integrated SOFC-fuel processing system for aircraft Propulsion," *Journal of Fuel Cell Science and Technology,* vol. 9, n° 4, pp. 041006 (8 pages), 2012. doi: 10.1115/1.4005587.

[10] D. F. Waters, "Modeling of gas turbine - solid oxide fuel cell systems for combined propulsion and power on aircraft (Ph.D. Thesis)," University of Maryland, College Park, Maryland, USA, 2015.

[11] M. Santin, A. Traverso and A. F. Massardo, "Technological aspects of gas turbine and fuel cell hybrid systems for aircraft: a review," *The Aeronautical Journal,* vol. 112, n° 1134, pp. 459-467, 2008. doi: 10.1017/S0001924000002426.

[12] J. A. Wilson et al., "Hybrid Solid Oxide Fuel Cell/Gas Turbine Model Development for Electric Aviation," *Energies,* vol. 15, n° 18, p. 2885, 2022. doi: 10.3390/en15082885.

[13] H. Hawa, S. Roychoudhury and C. Junaedi, "Hybridized, High Pressure, Liquid Fueled Solid Oxide Fuel Cell (SOFC) for Aircraft Primary Power," in *IEEE Transportation Electrification Conference and Expo*, Anaheim, CA, USA, 2022, pp. 1051-1056, doi: 10.1109/ITEC53557.2022.9813817.

[14] T. Mashamba et al., "Characteristic Investigation of a Novel Aircraft SOFC/GT Hybrid System under Varying Operational Parameters," *Applied Sciences,* vol. 14, n° 8, pp. 3504, 2024. doi: 10.3390/app14083504.

[15] K. Alsamri et al., "Dynamic modeling of Hydrogen SOFC/GT powered Aircraft with integration analysis," in *AIAA SciTech Forum and Exposition*, Orlando, FL, USA, 2024. Paper No: 2024-1532. doi: 10.2514/6.2024-1532.

[16] G. Agnew et al., "The Design and Integration of the Rolls-Royce Fuel Cell Systems 1MW SOFC," in *ASME Turbo Expo 2005: Power for Land, Sea, and Air*, Reno, Nevada, USA, 2005. Paper No: GT2005-69122, pp. 801-806. doi: 10.1115/GT2005-69122.

[17] Mitsubishi Power, "MHPS wins first order for integrated SOFC/gas turbine hybrid unit," [Online]. Available: https://power.mhi.com/news/20180131.html. [Accessed the 2 December 2024].

[18] R. A. George, "Status of tubular SOFC field unit demonstrations," *Journal of Power Sources*, vol. *86,* n° 1-2, pp. 134-139, 2000. doi: 10.1016/S0378-7753(99)00413-9.

[19] K. Huang and S. C. Singhal, "Cathode-supported tubular solid oxide fuel cell technology: A critical review," *Journal of power sources,* vol. *237,* pp. 84-97, 2013. doi: 10.1016/j.jpowsour.2013.03.001.

[20] K. Hassmann, "SOFC power plants, the Siemens-Westinghouse approach," *Fuel Cells,* vol. *1,* n° *1,* pp. 78-84, 2001. doi: 1615-6846/01/0105-78.

[21] F. J. Gardner et al., "SOFC technology development at Rolls-Royce," *Journal of Power Sources,* vol. *86,* n° *1-2,* pp. 122-129, 2000. doi: 10.1016/S0378-7753(99)00428-0.

[22] S. Pirou et al., "Production of a monolithic fuel cell stack with high power density," *Nature Communications,* Paper No: 1263, 2022. doi: 10.1038/s41467-022-28970-w.

[23] S. C. Singhal, "Solid oxide fuel cells for stationary, mobile, and military applications," *Solid State Ionics,* vol. *152*-153, pp. 405-410, 2002. doi: 10.1016/S0167-2738(02)00349-1.

[24] M. Kornely et al., "Degradation of anode supported cell (ASC) performance by Cr-poisoning," *Journal of Power Sources,* vol. 196, n° 17, pp. 7203-7208, 2011. doi: 10.1016/j.jpowsour.2010.10.033.

[25] C. Grosselindemann et al., "Pressurized single cell testing of solid oxide cells," *Journal of Power Sources,* vol. 641, pp. 234963, 2024. doi: 10.1016/j.jpowsour.2024.234963.

[26] D. E. Tew et al., "Perspective — the role of solid oxide fuel cells in our carbon-neutral future," *Journal of The Electrochemical Society,* 2022. doi: 10.1149/1945-7111/ac4ea3.

[27] B. Timurkutluk et al., "A review on cell/stack designs for high performance solid oxide fuel cells," *Renewable and Sustainable Energy Reviews,* vol. *56*, pp. 1101-1121, 2016. doi: 10.1016/j.rser.2015.12.034.

[28] T. A. Adams et al., "Energy conversion with solid oxide fuel cell systems: A review of concepts and outlooks for the short-and long-term," *Industrial & Engineering Chemistry Research,* vol. 52, n° *9*, pp. 3089-3111, 2013.

[29] D. Udomsilp et al, "Metal-supported solid oxide fuel cells with exceptionally high power density for range extender systems," *Cell Reports Physical Science,* vol. 1, n° *6*, pp. *100072*, 2020. doi: 10.1016/j.xcrp.2020.100072.

[30] B. W. Chung et al., "Development and characterization of a high performance thin-film planar SOFC stack," *Journal of the Electrochemical Society,* vol. 152, n° 2, pp. A265, 2004. doi: 10.1149/1.1843551.

[31] N. Droushiotis et al., "Comparison between anode-supported and electrolyte-supported Ni-CGO-LSCF micro-tubular solid oxide fuel cells," *Fuel Cells,* vol. 14, pp. 200-211, 2014. doi: 10.1002/fuce.201300024.

[32] J. Janikovic, "Gas turbine transient performance modeling for engine flight path cycle analysis", PhD thesis, School of Engineering, Cranfield University, UK, 2010. [Online]. Available: https://dspace.lib.cranfield.ac.uk/bitstream/handle/1826/7894/Jan_Janikovic_Thesis_2010.pdf.

[33] W. L. McMillan, "Development of a Modular Type Computer Program for the Calculation of Gas Turbine Off-Design Performance", PhD thesis, Cranfield Institute of Technology, UK, 1974. [Online]. Available: http://dspace.lib.cranfield.ac.uk/handle/1826/7401.

[34] P. P. Walsh and P. Fletcher, Gas Turbine Performance, 2nd ed., John Wiley & Sons, 2004.

[35] J. Linstrom and W. G. Mallard, "The NIST Chemistry WebBook: A Chemical Data Resource on the Internet," National Institute of Standards and Technology, 1 September 2001. [Online]. Available: https://doi.org/10.18434/T4D303. [Accessed the 9 Decembre 2024].

[36] M. Henke et al., "Influence of Pressurisation on SOFC Performance and Durability: A Theoretical Study," *7th Symposium on Fuel Cell Modelling and Experimental Validation (MODVAL),* vol. 11, n° 14, pp. 581-591, doi: 10.1002/fuce.201000098, 23rd-24th March 2011.

[37] X. Tong, Y. Wang et Y. Shi, "Sizing design and simulation of An SOFC propulsion system for unmanned aerial vehicles," in *ECS Transactions*, vol. 103, n° *1*, pp. 785, 2021. doi: 10.1149/10301.0785ecst.

[38] F. Trasino et al., "Modeling and performance analysis of the Rolls-Royce fuel cell systems limited: 1 MW plant," *Journal of Engineering for Gas Turbines and Power,* vol. 133, n° 2, pp. 1021701, 2011. doi: 10.1115/1.4000600.

[39] M. Ferrari et al., "Early start-up of solid oxide fuel cell hybrid systems with ejector cathodic recirculation: Experimental results and model verification," in *Proceedings of the Institution of Mechanical Engineers, Part A,* vol. 221, n° 5, pp. 627-635, 2007. doi: 10.1243/09576509JPE.

[40] K. Mathioudakis, "Evaluation of steam and water injection effects on gas turbine operation using explicit analytical relations," in *Proceedings of the Institution of Mechanical Engineers, Part A: Journal of Power and Energy*, vol. 216, n° 6, pp. 419-431, 2002. doi: 10.1243/095765002761034195.